

## EFFECT OF GADOLINIUM IONS ON STRUCTURAL AND OPTICAL PROPERTIES OF ZINC BOROTELLURITE GLASSES

Eevon Chua, Halimah Mohamed Kamari,  
Azmi Zakaria and Che Azurahaman Che Abdullah

*Department of Physics, Faculty of Science, Universiti Putra Malaysia,  
43400 UPM Serdang, Selangor, Malaysia*

*Corresponding author: halimahmk@upm.edu.my*

### ABSTRACT

Glasses with composition  $\{[(\text{TeO}_2)_{0.7}(\text{B}_2\text{O}_3)_{0.3}]_{0.7}(\text{ZnO})_{0.3}\}_{1-x}(\text{Gd}_2\text{O}_3)_x$ , where  $x = 0.01, 0.02, 0.03, 0.04$  and  $0.05$  mol have been fabricated by using conventional melt-quenching method. The structural properties of the prepared glass were determined via X-ray diffraction (XRD) analysis and Fourier transform infrared (FTIR) analysis. It was confirmed that the prepared glasses are all in amorphous nature. The FTIR analysis shows structural change from  $\text{TeO}_3$  to  $\text{TeO}_4$  and  $\text{BO}_4$  to  $\text{BO}_3$ . The optical absorption was recorded at room temperature in the wavelength ranging from 200 to 1000 nm. From the absorption edge data, the value of optical band gap  $E_{\text{opt}}$  and the Urbach energy  $\Delta E$  were evaluated and were found to be dependent on the composition of the glass.

### Highlights

- $\text{Gd}^{3+}$  affect the behaviour of optical absorption
- The FTIR study shows that there are changes in the structural units of the glass system
- The behaviour of Urbach energy is dependent on the composition of the glass

*Keywords: Gadolinium ion; Borotellurite glass; Optical band gap; Urbach energy;*

### INTRODUCTION

The development of gadolinium doped glasses have attracted a great deal of scientific interest due to their unique properties such as mechanical resistance, enhanced magnetic properties, higher chemical durability and photo-induced non-linear optical properties resulted from substantial contribution of anharmonic electron-phonon interactions [1-4]. The magnetic properties are determined by the present of gadolinium ions. Ristoiu et al. (1999) shows that the electron paramagnetic resonance (EPR) and magnetic susceptibility measurements performed on certain glasses containing gadolinium ions reveal aspects concerning to the distribution of gadolinium ions in the glass matrix and their microenvironment as well as the nature of magnetic interactions between ions [3-5]. These unique properties of studied glasses possess potential applications such as fast

ion conducting glasses, layers for optical and optoelectronics devices and thermal sensors [3].

In the previous study, there is not much information on the effect of gadolinium ions on the structural and optical properties on zinc borotellurite glass. Rada et al. (2008b) shows that gadolinium ions have influence on the homogeneity and stability of borotellurite glasses [6]. There is antiferromagnetic interactions between gadolinium ions distributed in the glass system as reported by [4].

The objectives of this present work are to study the effect of  $Gd_2O_3$  concentrations on the structural and optical properties by using X-ray diffraction (XRD) analysis, fourier transform infrared (FTIR) analysis and UV-Vis spectroscopic measurements.

## EXPERIMENTAL

Glasses with composition  $\{[(TeO_2)_{0.7}(B_2O_3)_{0.3}]_{0.7}(ZnO)_{0.3}\}_{1-x}(Gd_2O_3)_x$ , where  $x = 0.01, 0.02, 0.03, 0.04$  and  $0.05$  mol were prepared by using conventional melt-quenching method. The raw materials used to fabricate gadolinium zinc borotellurite glasses are tellurium oxide,  $TeO_2$  (Alfa Aesar, 99.99%), boron oxide,  $B_2O_3$  (Alfa Aesar, 97.5%), zinc oxide, ZnO (Alfa Aesar, 99.99%) and gadolinium oxide,  $Gd_2O_3$  (Alfa Aesar, 99.999%). Each chemical component used was weighed and mixed homogeneously using mortar and pestle.

Finely mixed powder were transferred into clean alumina crucible and transferred to a furnace that were preheated at  $400\text{ }^\circ\text{C}$  to remove moisture inside the mixtures. The mixtures were melted in a furnace at  $900\text{ }^\circ\text{C}$  and cast into a stainless steel cylindrical shaped split mould that had been preheated at  $350\text{ }^\circ\text{C}$  for to avoid thermal shock. The samples were annealed at  $400\text{ }^\circ\text{C}$  for 1 hour to remove thermal stress during quenching. The samples were cut into thickness of 2 to 3 mm each and were polished by using sandpaper to ensure the glass sample surface is parallel. The excessive glass sample was crush and ground further into finer powder.

The non-crystalline behaviour of the glass samples were tested using X-ray diffraction (XRD) analysis and Fourier Transform Infrared Spectroscopy (FTIR) analysis was used to study the structure of glass. The measurement of optical absorption edge in UV range was carried out using Camspec UV350 Visible Spectrophotometer at room temperature. The wavelength used in the measurement range from 200 nm to 1000 nm.

## RESULTS AND DISCUSSION

### X-ray Diffraction (XRD) Analysis

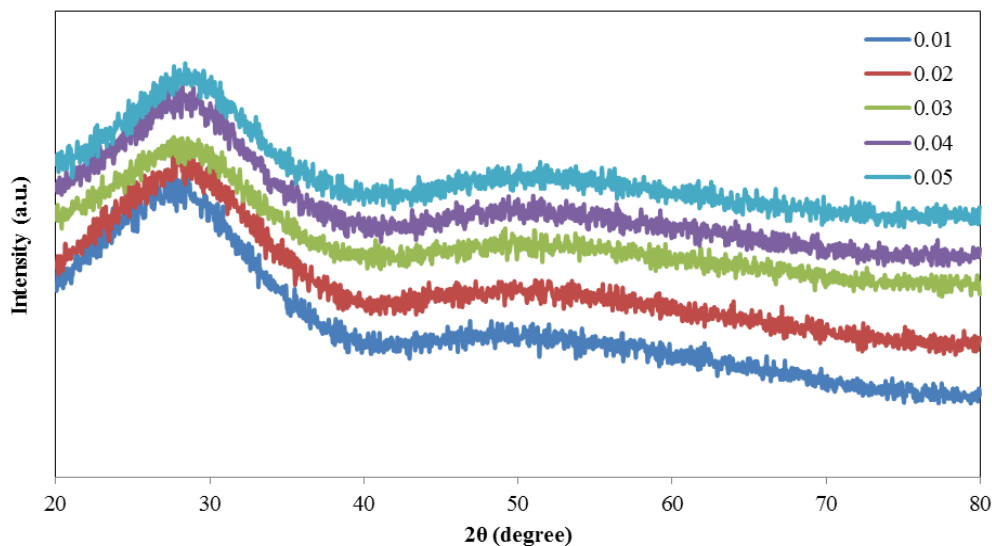


Figure 1: X-ray Diffraction Pattern of Gadolinium Zinc Borotellurite Glasses

The X-ray diffraction patterns of the gadolinium zinc borotellurite glass samples  $\{[(\text{TeO}_2)_{0.7}(\text{B}_2\text{O}_3)_{0.3}]_{0.7}(\text{ZnO})_{0.3}\}_{1-x}(\text{Gd}_2\text{O}_3)_x$  are shown in Figure 1. Figure 1 shows similar patterns that do not reveal any distinguishable peaks or sharp lines. The x-ray diffraction patterns exhibit a broad hump at low angle which shows the absence of long range structural order in the glass samples. The absence of discrete or distinguish sharp peaks indicate that the prepared glass samples were amorphous in nature [7,8].

### Fourier Transform Infrared Spectra (FTIR)

The fourier transform infrared (FTIR) Spectra of Gadolinium Zinc Borotellurite  $\{[(\text{TeO}_2)_{0.7}(\text{B}_2\text{O}_3)_{0.3}]_{0.7}(\text{ZnO})_{0.3}\}_{1-x}(\text{Gd}_2\text{O}_3)_x$  glass system in the frequency range from 400 to 4000  $\text{cm}^{-1}$  is shown in Figure 2. The infrared transmission bands are assigned based on the literature data on the wavenumber ranges that are related to the corresponding vibrations of the structural units in various glass systems. From Figure 2, the infrared transmission bands of present glasses are summarized in Table 1.

Figure 2 shows two significant IR absorption regions around 640-653  $\text{cm}^{-1}$  and 1229-1237  $\text{cm}^{-1}$ . At  $x = 5$  mol%, there exists a band around 905  $\text{cm}^{-1}$ . It is clearly shown that the absorption band around 640-653  $\text{cm}^{-1}$  are attributed to stretching vibrations of  $\text{TeO}_4$  trigonal bipyramid units as reported [6, 10]. As a result, the formation of non-bridging oxygen decrease as the concentration of  $\text{Gd}_2\text{O}_3$  increases. The addition of  $\text{Gd}_2\text{O}_3$  to the glass network may form Gd-Te-O, Gd-O-Te or Gd-O-Gd bonds in place of Te-O-Te linkages.

Whereas, the absorption band around  $1229-1237\text{ cm}^{-1}$  corresponding to B-O stretching vibrations in  $\text{BO}_3$  units from boroxol rings while the absorption bands at  $x = 5\text{ mol\%}$  are due to stretching of B-O bonds of  $\text{BO}_4$  units as reported. Besides, it could be attributed to the formation of bridging bond of Te-O-B. This is because the stretching force constant of Te-O bonding is substantially lower than that of B-O. Hence, the stretching frequency of Te-O-B might tend to be lower [9, 11].

Table 1: Assignment of infrared transmission bands of Gadolinium Zinc Borotellurite,  $\{[(\text{TeO}_2)_{0.7}(\text{B}_2\text{O}_3)_{0.3}]_{0.7}(\text{ZnO})_{0.3}\}_{1-x}(\text{Gd}_2\text{O}_3)_x$  glasses

No.	Band position	Assignments
1.	$640-653\text{ cm}^{-1}$	$\text{TeO}_4$ groups presences in all tellurite containing glass [12-13]
2.	$\sim 905\text{ cm}^{-1}$	Stretching of B-O bonds of $\text{BO}_4$ units [9]
3.	$1229-1237\text{ cm}^{-1}$	Trigonal B-O bond stretching vibrations of $\text{BO}_3$ units from boroxyl groups [12]

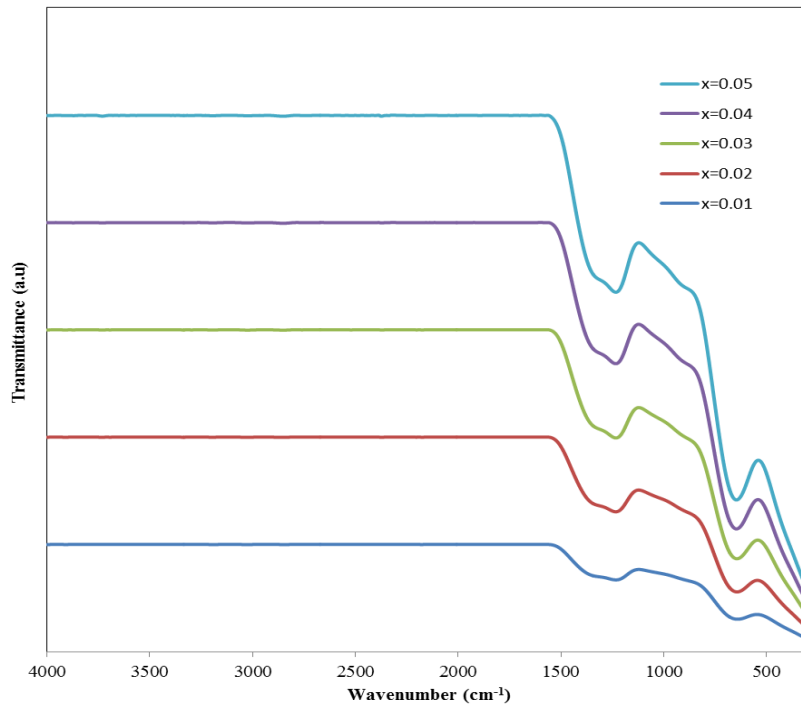


Figure 2: FTIR Transmittance Spectra of Gadolinium Zinc Borotellurite,  $\{[(\text{TeO}_2)_{0.7}(\text{B}_2\text{O}_3)_{0.3}]_{0.7}(\text{ZnO})_{0.3}\}_{1-x}(\text{Gd}_2\text{O}_3)_x$  glasses

### UV-Vis Spectra

The studies on optical absorption of a material give information on optical absorption coefficient, direct and indirect optical band gap and Urbach energy. The absorption coefficient,  $\alpha$  show the ability of a material to absorb light of a given wavelength can be calculated from the following relation:

$$\alpha(\omega) = 2.303 \frac{A}{d} \quad (1)$$

where A is the absorbance and d denotes to the thickness of the glass samples [14].

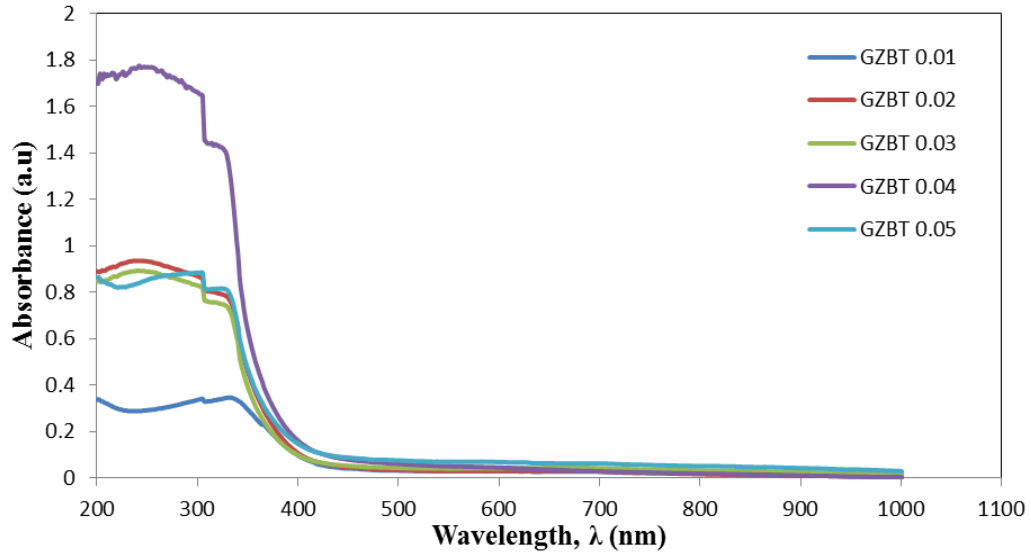


Figure 3: Optical Absorbance Spectra for Gadolinium Zinc Borotellurite Glasses

Figure 3 shows the optical absorption edges of the present glass materials. It found that the optical absorption edges are not sharply defined which shows the characteristics of amorphous materials. The results obtained are in agreement with the x-ray diffraction results in Figure 1. The change in the characteristics of the absorption edge is due to the change in the oxygen bonding of the glass network. The fundamental edge shifts to lower wavelength as the concentration of  $Gd_2O_3$  increases. The shift of absorption edge can be attributed to the decrease in non-bridging oxygen, structural rearrangement of glass and relative concentration of various fundamental units. The presence of  $TeO_4$  in the present glass network causes formation of bridging oxygen atom which cause decrease in non-bridging oxygen [12, 14-15].

### Optical band gap

The relationship between absorption coefficient  $\alpha(\omega)$  as a function of photon energy  $\hbar\omega$  for both direct and indirect transition is given by the following equation:

$$\alpha(\omega) = \frac{A(\hbar\omega - E_{opt})^n}{\hbar\omega} \quad (2)$$

where A is constant,  $E_{opt}$  is the energy of optical band gap,  $\hbar\omega$  is the photon energy and  $\alpha(\omega)$  is the absorption coefficient. The values of n is an index depending on the nature

of interband transitions where  $n = 1/2$  for allowed direct transition and  $n = 2$  for allowed indirect transitions [10, 16-17].

The relationship between  $(\alpha\hbar\omega)^2$  versus photon energy ( $\hbar\omega$ ) and  $(\alpha\hbar\omega)^{1/2}$  versus photon energy ( $\hbar\omega$ ) are plotted as shown in Figure 4 and Figure 5, respectively. The values of optical band gap ( $E_{opt}$ ) for either direct or indirect can be obtained by extrapolating  $(\alpha\hbar\omega)^2$  and  $(\alpha\hbar\omega)^{1/2}$  equal to zero. The values of optical band gap energy obtained are tabulated in Table 2.

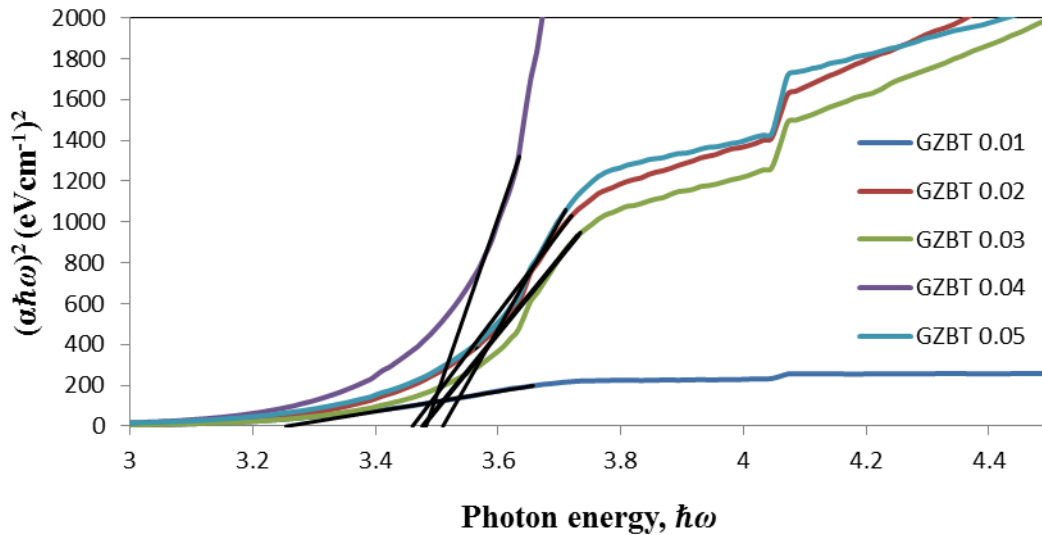


Figure 4: Direct Energy Band Gap of Gadolinium Zinc Borotellurite Glasses

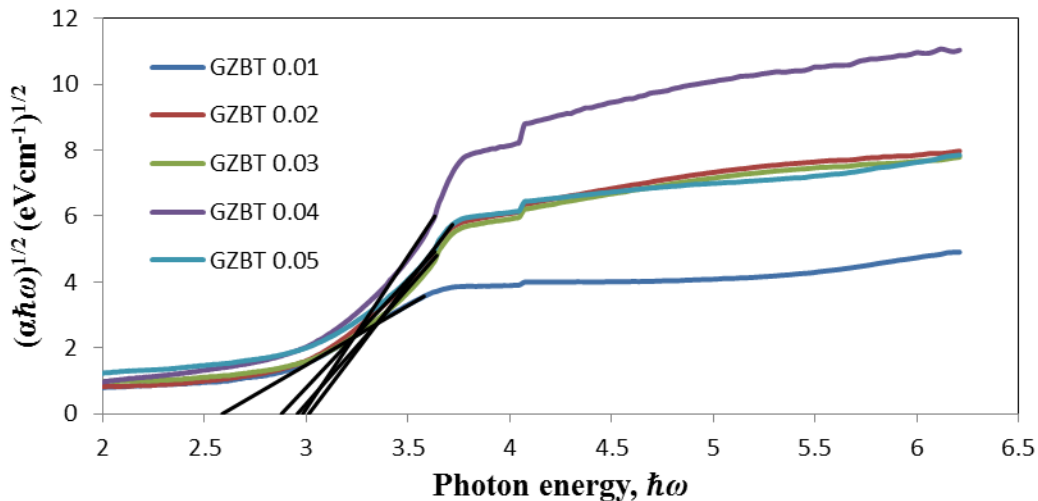


Figure 5: Indirect Energy Band Gap of Gadolinium Zinc Borotellurite Glasses

Table 2: Direct Energy Band Gap,  $E_{opt}^1$  Indirect Energy Band Gap,  $E_{opt}^2$  and Urbach Energy ( $\Delta E$ ) of Gadolinium Zinc Borotellurite Glasses

Mole fraction, x	Direct energy band gap, $E_{opt}^1$ (eV)	Indirect energy band gap, $E_{opt}^2$ (eV)	Urbach Energy, $\Delta E$ (eV)
0.01	3.254	2.587	0.323
0.02	3.460	2.878	0.328
0.03	3.477	2.957	0.327
0.04	3.482	2.984	0.344
0.05	3.510	3.013	0.344

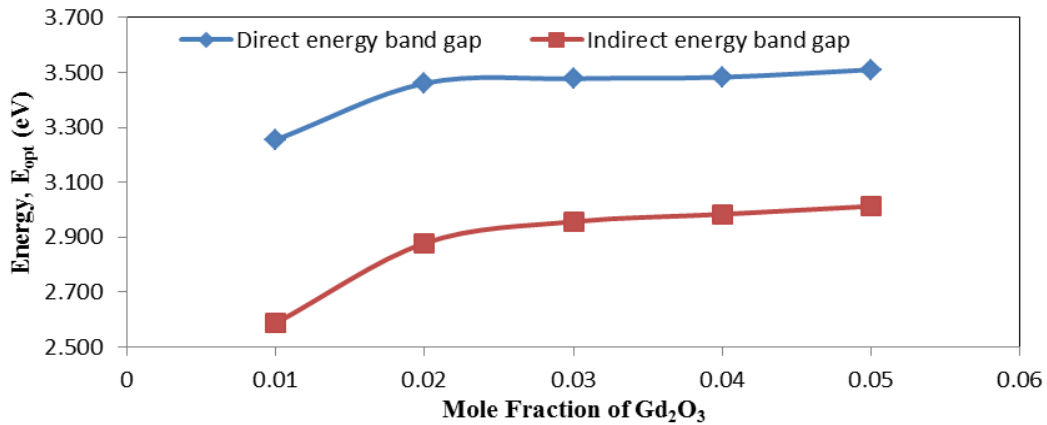


Figure 6: Variation of Direct and Indirect Optical Band Gap with Glass Composition for Direct and Indirect Transition for Gadolinium Zinc Borotellurite Glasses

The values of direct and indirect energy band gap increases from 3.254 to 3.510 eV and from 2.587 to 3.013 eV respectively. The increase in direct and indirect energy band gap is due to structural rearrangement of the glass network after addition of Gd<sub>2</sub>O<sub>3</sub> [1, 18]. Introduction of Gd<sup>3+</sup> ions into the glass network would cause a decrease in the degree of electrons localization thereby decrease the donor centers in the glass matrix which leads to increase in optical energy gap. After addition of Gd<sub>2</sub>O<sub>3</sub>, the structure in the glass network changes by transforming TeO<sub>3</sub> to TeO<sub>4</sub> forming bridging oxygen which leads to increase in optical band gap. Electrons in bridging oxygen are tightly bound as compared to that in non-bridging oxygen atoms. The magnitude of negative charge on bridging oxygen is less than that on non-bridging oxygen atoms. Therefore, an increase in bridging oxygen atoms causes a decrease in ionicity of oxygen ions and hence lowering the top of valence band and leads to increase in optical band gap [1,19]. Decreasing number of non-bridging oxygen atoms show that the number of free electrons in the glass network decreases. Besides, the band gap values of Gd<sub>2</sub>O<sub>3</sub> (5.4eV) is higher than that of TeO<sub>2</sub>-B<sub>2</sub>O<sub>3</sub>-ZnO (3.28eV). This suggests that the band gap values increases when lower band gap contents are replace by higher band gap contents in the

glass system [20]. The increase in the direct and indirect energy band gap for the glass system can be related to the variation of density as well as electronic defects and breaks in the vitreous network bonds which allow the glass structure to relax and fill the relative large interstices that exist in the interconnected network of boron, tellurium and oxygen atoms causing expansion followed by compaction of the volume [21-23].

#### *Urbach energy*

Urbach energy,  $\Delta E$  is the band tails associate with the valence and conduction band which extend into the forbidden energy band gap. It is used characterize the degree of disorder as well as the number of defects in materials. The absorption coefficient varies in accordance to Urbach's rule as the following relation:

$$\alpha(\omega) = A \exp(\hbar\omega/\Delta E) \quad (4.6)$$

Here A is a constant;  $\Delta E$  is known as Urbach energy which corresponds to the width of the localized states. Urbach energies are calculated from the reciprocal slopes of the linear portion from  $\ln \alpha$  versus photon energy plots [11, 24-25]. The data obtained are recorded in Table 2. Urbach energies of the studied glass range from 0.323-0.344 eV. The Urbach energies of the present glass are in range of amorphous semiconductor 0.045 and 0.567 eV [15]. The values of Urbach energies increase as the concentration of  $Gd_2O_3$  increases. This suggests that there is high degree of disorder in glass system and the defects which act as the nuclei for crystallization increases as the concentration of  $Gd_2O_3$  increases [15,19]. This is due to low crystallization temperature as a result of rapid nucleation process hence causing the studied glass to become less stable. Hence, the increasing values of Urbach energy  $\Delta E$  with increasing concentration of  $Gd_2O_3$  content shows that the fragility nature of the vitreous network to increase.

## CONCLUSION

X-ray diffraction and FTIR spectroscopy have been used to study the structural changes produced by the variation of  $Gd_2O_3$  concentration in  $\{[(TeO_2)_{0.7}(B_2O_3)_{0.3}]_{0.7}(ZnO)_{0.3}\}_{1-x}(Gd_2O_3)_x$  glass systems. X-ray diffraction patterns show that the present glasses are amorphous in nature. FTIR spectroscopy shows decreasing formation of non-bridging oxygen as the concentration of  $Gd_2O_3$  increases. UV-vis absorption spectra had been used to study the optical properties of present glass systems. The optical absorption edges do not show any sharp absorption edges which indicate that the prepared glass samples are amorphous in nature. The increase in direct and indirect energy band gap is due to structural rearrangement, higher band gap values of  $Gd_2O_3$  (5.4eV), variation of density as well as electronic defects and breaks in the vitreous network bonds. Therefore, it may be concluded that the present glass system undergoes structural changes with the addition of  $Gd_2O_3$  as network modifier.

## ACKNOWLEDGMENTS

The authors appreciate the financial support for the work from Universiti Putra Malaysia through GPIBT (9411800).

## REFERENCES

- [1] Luo, H., Hu, X., Liu, W., Zhang, Y., Lu, A., & Hao, X. *Journal of Non-Crystalline Solids*, **389** 86–92 (2014)
- [2] Liang, X., Li, H., Wang, C., Yu, H., Li, Z., & Yang, S. *Journal of Non-Crystalline Solids*, **402** 135–140 (2014)
- [3] Saddeek, Y. B., Yahia, I. S., Aly, K. A., & Dobrowolski, W. *Solid State Sciences*, **12** (8) 1426–1434 (2010)
- [4] Ristoiu, T., Culea, E., & Bratu, I. *Materials Letters*, **41** (3) 135–138 (1999)
- [5] Rada, S., Pascuta, P., Bosca, M., Culea, M., Pop, L., & Culea, E. *Vibrational Spectroscopy*, **48** (2), 255–258 (2008)
- [6] Rada, S., Culea, E., Bosca, M., Culea, M., Pascuta, P., & Neumann, M. *Journal of Optoelectronics and Advanced Materials*, **10** (9), 2316–2318 (2008)
- [7] Yang, F., Huang, B., Wu, L., Peng, S., Qi, Y., & Zhou, Y. *Journal of Quantitative Spectroscopy and Radiative Transfer*, **161** 1–10 (2015)
- [8] Stambouli, W., Elhouichet, H., & Ferid, M. *Journal of Molecular Structure*, **1028** 39–43 (2012)
- [9] Rada, S., Culea, E., Rada, M., Maties, V., Bosca, M., Pop, L., Fechete, R., Chelcea, R., & Moldovan, D. *Journal of Physics: Conference Series*, **182** 012075 (2009)
- [10] Kundu, R. S., Dhankhar, S., Punia, R., Nanda, K., & Kishore, N. *Journal of Alloys and Compounds*, **587** 66–73 (2014)
- [11] Suthanthirakumar, P., Karthikeyan, P., Manimozhi, P. K., & Marimuthu, K. *Journal of Non-Crystalline Solids*, **410** 26–34 (2015)
- [12] Azlan, M.N., Halimah, M.K., Siti Shafinas, Z. and Daud, W.M. *Journal of Nanomaterials*, Volume 2013, Article ID 940917 (2013)
- [13] Gayathri Pavani, P., Sadhana, K., & Chandra Mouli, V. *Physica B: Condensed Matter*, **406** (6-7) 1242–1247 (2011)
- [14] Edukondalu, A., Rahman, S., Ahmmad, S. K., Gupta, A., & Siva Kumar, K. *Journal of Taibah University for Science* **10** (3) 363–368 2016
- [15] Veeranna Gowda, V. C. *Physica B: Condensed Matter*, **456** 298–305 (2015)
- [16] Ghribi, N., Dutreilh-Colas, M., Duclère, J.-R., Hayakawa, T., Carreaud, J., Karray, R., Kababou, A., & Thomas, P. *Journal of Alloys and Compounds*, **622** 333–340 (2015)
- [17] Maheshvaran, K., & Marimuthu, K. *AIP Conference Proceedings*, 1349 (PART A), 581–582 (2011)
- [18] Mhareb, M. H. A., Hashim, S., Ghoshal, S. K., Alajerami, Y. S. M., Saleh, M. A., Dawaud, R. S., Razak, N. A. B., & Azizan, S. A. B. *Optical Materials*, **37** 391–397 (2014)
- [19] Singh, S., & Singh, K. *Journal of Non-Crystalline Solids*, **386** 100–104 (2014)
- [20] Sreenivasulu, V., Upender, G., Chandra Mouli, V., & Prasad, M. *Spectrochimica Acta. Part A, Molecular and Biomolecular Spectroscopy*, **148** 215–222 (2015)

- [21] Rao, S. L. S., Ramadevudu, G., & Hameed, A. *International Journal of Engineering, Science and Technology*, **4** (4), 25–35 (2012)
- [22] Patil, S.D. and Jali, V.M. Optical properties of Neodymium doped Borotellurite glasses. *International Journal of Science Research* **1** (4) 317-320 (2012)
- [23] Mustafa, I. S., Kamari, H. M., Wan Yusoff, W. M. D., Aziz, S. A., & Rahman, A. A. *International Journal of Molecular Sciences*, **14** (2), 3201–3214 (2013)
- [24] Farouk, M., Abd El-Maboud, A., Ibrahim, M., Ratep, A., & Kashif, I. *Spectrochimica Acta. Part A, Molecular and Biomolecular Spectroscopy*, **149** 338–342 (2015)
- [25] Elkhoshkhany, N., Abbas, R., El-Mallawany, R., & Fraih, A. J. *Ceramics International*, **40** (9), 14477–14481 (2014)